FTD-ID(RS)T-0735-82

FOREIGN TECHNOLOGY DIVISION

VOLTAGE BREAKDOWN OF SPARK GAPS IN COMPRESSED GASES

by

W. Pfeiffer

EDITED TRANSLATION

FTD-ID(RS)T-0735-82 7 June 1982

MICROFICHE NR: FTD-82-C-000739

VOLTAGE BREAKDOWN OF SPARK GAPS IN COMPRESSED GASES

By: W. Pfeiffer

English pages: 19

Source: Zeitshrift fur Angewante Physik, Nr. 4, 1971, pp. 265-273

Country of origin: East Germany
Translated by: TSgt Michael L. Seidel
Requester: FTD/TQTD
Approved for public release; distribution unlimited.

GRAPHICS DISCLAIMER

All figures, graphics, tables, equations, etc. merged into this translation were extracted from the best quality copy available.

VOLTAGE BREAKDOWN OF SPARK GAPS IN COMPRESSED GASES

W. Pfeiffer

Institute for High Voltage and Measurement Technology of the Darmstadt Technical College

Submitted 22 Jan 1971, Finalized 15 July 1971

The validity of the three spark laws of Toepler, Rompe-Weizel and Braginskii is checked in a wide range of gap width, pressure and kind of gas. Only the time interval of the voltage breakdown at the spark gas is regarded. The measurements show, that all spark laws are useful on these conditions. The highest accuracy and the easiest applicability are attained using the spark law of Toepler.

1. Introduction

The so-called spark laws describe the time progression of the electrical magnitudes during spark discharges, and preferably in the realm of the fast voltage breakdown. However, the applicability of these laws are made difficult by the fact that there are constants present in all of them, whose numerical value cannot be calculated from the properties of the gas involved. Therefore, it is the goal of this work, to determine spark constants experimentally in as wide a range as possible. Thereby, in particular, the still extensively unexamined region for high gas pressure is to be obtained. The voltage breakdown times to be expected in the range of a few

nanoseconds require a correspondingly high bandwidth of the test assembly, whereby the achievable test voltage is decisively limited.

2. Spark Laws and Spark Constants

First to be mentioned is Teopler's Spark Law, which was established by Toepler [1] purely empirically. The high accuracy of the law signifies the fact that a true correlation with the processes in the spark channel can be established. A test on this to date is available only from Toepler [3]. Here, the law should at least be traced back formally on a model representation concerning the development of the spark channel. For this, as for the other theories, it is assumed that the ignition of the discharge has already taken place and a weakly conducting plasma channel exists, whose conductance is to be increased by shock ionization

$$dn_e = n_e \cdot \varphi_{ion} \cdot dx \qquad (1)$$

n_e - concentration of electrons, φ_{ion} - effective cross section for ionization, dx - distance traveled by the electrons.

The distance can be determined through the velocity

$$v_e = b_e \cdot E, \quad dx = b_e \cdot E \cdot dt. \qquad (2)$$

v_e - velocity of the electrons, b_e - mobility of the electrons, E - mean field strength along the spark channel.

Through introduction of the current density there results

$$j = n_e \cdot b_e \cdot e \cdot E, \quad dn_e = \frac{\varphi_{ion}}{e} \cdot j \cdot dt. \qquad (3)$$

j - mean current density in the spark channel, e - elementary charge.

Thereby at time t after the nominal start of the spark discharge an electron concentration is obtained as:

$$n_{e,t} = \frac{\varphi_{ion}}{e} \cdot \int_0^t j \cdot dt. \qquad (4)$$

Now the Ohm's resistance R_f of the spark channel which is to be assumed as homogeneous can be calculated as

$$R_{fo} = \frac{u}{i} = \frac{E \cdot s}{\pi \cdot r_f^2 \cdot E \cdot \eta} \quad \frac{s \cdot \eta \cdot q_m \cdot b_e \cdot \int i \cdot dt}{\pi \cdot r_f^2 \cdot q_m \cdot b_e \cdot \int i \cdot dt} \tag{5}$$

s - sparking distance of the spark gap length, r_f - radius of the spark channel.

From this is obtained the Toepler Law, if the track radius is assumed to be a time constant

$$R_{fo} = \frac{k}{q_m \cdot b_e \cdot \int i \cdot dt} \tag{6}$$

As an evaluation of the Toepler Spark Constants k, there results

$$k = b_e \cdot \frac{1}{q_m} \cdot \tag{7}$$

The omission of track expansion at air and normal pressure is presumably permissible until about 10 ns after the nominal start of the spark [9, 13].

Up to now measurement values for the spark constants k are available only for air and normal pressure. From the measurements of Andreev and Vanyukov [8], over a half wave of the oscillating discharge current there result mean values for the spark constants of $0.46\text{-}0.85 \cdot 10^{-4}$ Vs/cm. However, due to the long periodicity of maximally 160 ns and the artificial ignition of the spark gaps, these values are not particularly reliable. Heilbronner and Kaerner [12] by means of digital calculation of the voltage progression on spark gaps at a mean spark field strength E_0 of 20-30 kV/cm determine spark constants of $0.4\text{-}0.6 \cdot 10^{-4}$ Vs/cm. These data agree very well with the measurements by Moeller [13], which yielded spark constants between 0.45 and $0.65 \cdot 10^{-4}$ Vs.cm for spark field strengths of 15-30 kV/cm.

The spark law of Rompe and Weizel [4, 5] is based on quite similar assumptions to those of the theory conducted for Toepler's

Law. The most important agreements are the omission of track expansion and the prerequisite that the ions remain at rest. Thereby there also results for the spark resistance a similar expression

$$R_{sp} = \frac{\cdot}{\sqrt{\cdot \frac{\cdot}{\cdot} \int \cdot \cdot dt}} \qquad (8)$$

and as interpretation of the spark constants a

$$a = \frac{\cdot \cdot \cdot}{\frac{\cdot}{\cdot} \cdot \cdot \cdot + \cdot \cdot \left(\cdot + \frac{\cdot}{\cdot} \cdot \cdot \right)} \qquad (9)$$

p - gas pressure, k - Boltzmann constants, T_e - electron temperature, V_i - ionization potential, V_a - excitation potential, n_a - concentration of excited atoms.

In relation to the range of time validity of the law, the same considerations as for Toepler's Law apply.

Also, for the spark constants a, only measurement values for air are available. For short sparking distances at normal pressure a value of 1.1 atm·cm^2/V^{2}s was determined by Gruenberg [10]. The measurements by Moeller [13] at a spark field strength of E_0=30 kV/cm yield a value of 1.0 atm·cm^2/V^{2}s, which at a reduction of E_0 by utilization of hyberbolic electrodes to 15 kV/cm increases to 2.5 atm·cm^2/V^{2}s. An explanation for this behavior has yet to be given. For higher gas pressures of up to 7 atm, only the measurement values of Nesyats and Korshunov [14] are available which move between 0.5 and 1 atm·cm^2/V^{2}s, without showing a notable dependence on gas pressure.

In a totally different manner Braginskiy [7] arrived at a spark law, whereby the theory of Drabkina is further expanded [6]. Under the premise that the means with specific conductance of the spark track is independent of time, the time progression of the track radius can be calculated. From this there then yields the spark resistance

$$R_{sp} = \frac{\cdot}{\cdot \cdot \cdot \cdot \int \cdot \cdot dt} \qquad (10)$$

whereby $\kappa \cdot A^2$ is to be viewed as the support constants. For this the constants are yielded as follows:

$$\left.\begin{array}{l} A = \left[\dfrac{4}{\pi^2 \cdot \rho_0 \cdot \xi \cdot \kappa}\right]^{1/6}, \\ \xi = K_p \cdot \left[1 + \dfrac{1}{\gamma - 1} \cdot \left(2 - \dfrac{1}{\gamma}\right)\right], \\ r_{(t)} = A \cdot t ; \end{array}\right\} \qquad (11)$$

ρ_0 - gas density before the start of the discharge, κ - mean specific conductance of the spark track, K_p - resistance coefficient, γ - adiabatic coefficient, determined by approximation [6], $r_{(t)}$ - radius of the track shell.

The law is presumably valid over a large time range and only then fails when the omission of the energy losses is impermissible. During the voltage breakdown, in contrast, notable errors are to be expected, since here κ can assuredly not be assumed as constant.

Measurement values of the spark constants, to date, are only available for air and normal pressure. Under these conditions Andreev and Orlov [11] name a value of $4.3 \cdot 10^5$ $A^{1/3} \cdot cm/Vs$. The spark constants are determined by Moeller [13] at $4.5 \cdot 10^4$ $A^{1/3} \cdot cm/Vs$, in any case dependent on the magnitude of the discharged capacitance. A basis for this is yet to be given.

3. Measurement Processes and Solution of the Equation of the Discharge Circuit

As a measurement process the principle of the line discharge is used. For this a strip line or a coaxial line is charged to the static ignition voltage U_0 of the spark gap and then discharged over a series circuit of spark resistance and low-Ohm current-measuring resistance. Thereby the omission of inductance and capacitance is attempted, which leads to Fig. 1 as a simplified equivalent circuit diagram.

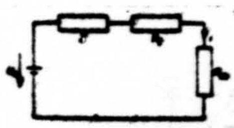

Fig. 1. Equivalent circuit diagram of the discharge circuit.

The equivalent circuit will be that much more valid the higher the characteristic resonance of the oscillatory circuit is formed from the spark inductance and electrode capacitance. The spark resistance which is sought can then immediately be given as

$$R_f \approx \frac{U_f}{I_f} - R_s \approx \frac{U_f}{I_f} \quad (12)$$

The error through the ignoring of R_m for the relatively high spark resistances considered here, is without significance. The maximal value of the discharge current results at

$$I_{max} = \frac{U_0}{R + R_f + R_s} \approx \frac{U_0}{R}. \quad (13)$$

During application of this approximation some 30 ns after the nominal spark begins at normal pressure an error of maximally 5% must be considered. From this it ensues that, from the oscillogram of the discharge current, the height of the breakdown voltage U_0 can be determined with good accuracy. Under application of equations (12), (13), the course of the discharge current under consideration of the various spark laws is to be calculated. For the Toepler Law after standardization of the discharge current the following is obtained

$$\begin{cases} \dfrac{dy}{dx} = y(1-y^2) & y_{max} \\ \dfrac{1}{2}\ln\dfrac{1+y}{1-y} + \dfrac{1}{y} = x - c \end{cases} \quad (14)$$

The corresponding solution for a voltage transient wave was already derived by Meuller [2]. The value of the integration constants is determined by the selection of the nominal spark begin and thus by the resolving power of the current measurement.

Also for the law by Rompe and Weizel a similar problem has already been solved [14]. Under the conditions existing here one obtains

$$\left[\quad\right] \quad (15)$$

The solution exhibits formally a certain similarity to that obtained for the Toepler Law.

Braginskiy's Law up to now has not yet been used for the calculation of line discharges. Here the following results:

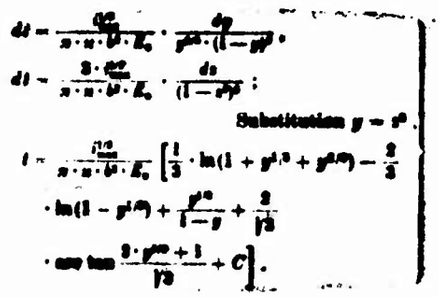

(16)

It has proven purposeful to define the nominal spark begin at y=0.01. Thus the following integration constants are obtained:

Toepler	Rompe and Weizel	Braginskiy
C=3.58	C=3.07	C=-1.25

The maximal current transconductance is yet to be determined from the obtained solutions. Therefrom a time t_{max} can then be defined, that an artificial key wave of equal maximal slope requires for current rise from y=0 to y=1 [14]

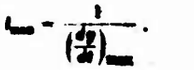

(17)

For the individual spark laws the following expressions are yielded:

Toepler

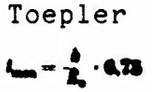

Rompe and Weizel

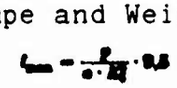

Braginskiy

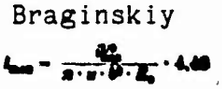

Through comparison of the individual values an additional control possibility of the spark laws among one another exists.

4. Assembly of the Measurement Facility

The test assembly is to correspond as exactly as possible in its properties to fig. 1. For this first a coaxial cable with a wave resistance which is real up to over 1 GHz and which is constant over the cable length is required. Type RG218/U (metal cable) with 90 kV is indicated as the only high frequency cable of the necessary dielectric strength, whereby the wave resistance amounts to 50 Ω.

The actual problem lies in the realization of the transition from cable to spark gaps. The solution selected is shown in Fig. 2.

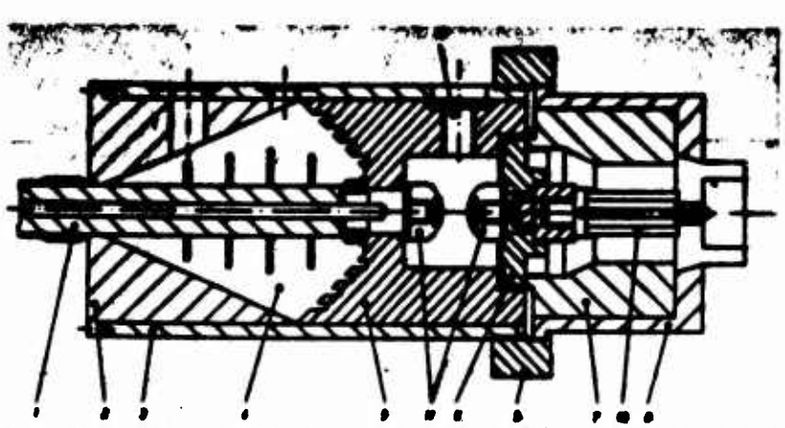

Fig. 2. Spark-gap distances and cable-end connection.

On the bases of dielectric strength and the special requirement for the spark-gap distances, thereby a greater cross section jump is unavoidable. It is attained by a conical transition section (2), which continues the external conductor of the cable (1) onto the external covering of the spark-gap distances (3). The hollow space (4) thus formed is filled with a silicon rubber (Silopren K1, Bayer). Ceramic (Stenan, Steatit-Magnesia) which was fired at 1200°C after molding, has proven itself to be reliable as the material for the spark chamber (5). As a result of the relatively low tensile strength of this material, the cover of the spark chamber must be prestressed over a bushing (7) by the pressfit fitting (8, 9). The current measurement resistor (12) was simultaneously built

into this. The gas to be examined is introduced radially (10). The electrodes (11) are approximately hemispherical and have tungsten caps for reduction of burnoff.

Current measurement was accomplished with the Tektronix 519 (T_a=0.29 ns; vertical 9.4 V/scalar unit) oscillograph. If a measurement range change by weakening of the signal occurs, then that leads very quickly to an overloading of the current measurement resistor. Therefore here exclusively the resistance value is changed. Coaxial tube resistors are very well suited for this [15]. The foil of NiCr 80/20 (Vacromium, vacuum molded) of 10 um thickness serves as the resistor element. Thus in the frequency range of interest up to 1 GHz the effect of current displacement on the transmission behavior can be disregarded. In contrast, the requirement that the length of the resistor tube must also still be disregardable compared to the smallest arriving wavelength, is of decive significance, whereby at most λ=3 cm may be permitted. The transmission behavior of the resistors employed was derived by measurement of the rectangular wave pulse resistance at test currents of up to 6 A, whereby a rise time of maximally 0.45 ns resulted. The circuitry of the overall test assembly is shown in Fig. 3.

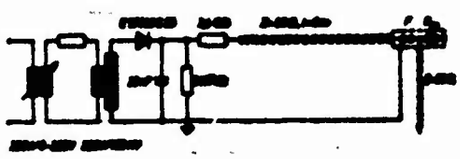

Fig. 3. Overall circuitry.

Thereby the compensating resistance of 2.4 ω provides for a sufficiently large charge time constant, so that between the discharges complete resolidification of the insulating gas takes place. The voltage tap on the current measurement equipment is accomplished with 50 Ω wave resistance, whereby the oscillogram is adapted over a closed T-member in the signal direction.

For determination of the transmission behavior of the overall equipment, a test with shorted electrodes and conduction of the test pulse to the pressurized gas connection was conducted. Thereby

there resulted the following square wave pulse response (Fig. 4).

Fig. 4. Square wave pulse response. Time sweep, 0.5 ns/scalar unit, measured with Tektronix [illegible].

With a rise time of 1.1 ns, the facility has a bandwidth of 320 MHz.

Naturally, the current rise is delayed by this finite bandwidth, whereby the error increases with an increase in ignition field strength E_0. For the critical case (N_2, E_0=310 kV/cm), from equation (14) at k=$0.5 \cdot 10^{-4}$ Vs/cm a rise time of the discharge current is calculated by

$$T_{\ddot{u}} = 13.3 \cdot \frac{k}{E_0} = 2.15\,\text{ns}. \qquad (18)$$

This value is enlarged by the limited bandwidth of the facility by about 12%. Further errors are still possible due to the effect of the electrode capacitance and the spark inductance. The contribution of the error with increasing ignition field strength also increases. The greatest ignition field strength occurs at the smallest spark gap and thus the greatest electrode capacitance. Thus the capacitative effect could dominate the inductive by far, which is also confirmed by a corresponding error estimation. Thereby, the maximal possible increase in discharge current amounts to 22%.

5. Measurements and Evaluations

In the course of the measurements, spark gap distances and gas pressures were changed as follows

a/mm	0.5	1	2	3	4	5	6	7	8	9	10
p/at	1.25[a]	1.5	2	2.5	3	3.5	4	4.5[a]	5	5.5[a]	6 7 8 9
	10[a]	11									

[a]Not examined for Argon.

As the filling gases served nitrogen, carbon dioxide, and argon in the purest form (Messer-Griesheim). It is to be noted, that the pressure measurement is accomplished here in technical atmospheres, and that the Rompe and Weizel spark constants thus obtain the dimension at·cm^2/V^{2}s in contrast to previous measurements.

The derivation of the breakdown voltages is accomplished according to equation (13) from the maximal value of the discharge current. The results agree well with the data of Gaenger [16]. For large values of p·s (maximally some 30 at·mm) it is shown that carbon dioxide exhibits some 87% and argon some 20% of the voltage strength of nitrogen.

The determination of the spark constants which are sought is accomplished by point-by-point comparison of the measured and the calculated current path for the standardized current values y=0.1; 0.2, ..., 0.9. Thereby, the arithmetic mean value is given as the actual spark constant. For the evaluation only the peak and maximal values of the current path which occurs, which Fig. 5 shows for negative polarity of the charge voltage, are required.

Fig. 5. Discharge current path s=2 mm, p=2 at, vertical 635 A/scalar unit, sweep time 20 ns/ scalar unit.

The progression of the spark constants during a discharge is shown now for a few characteristic parameter combinations (Figs. 6 and 7).

It is shown that for Toepler's Law almost a true constant exists. Up to a standardized current value of y≈0.5 that is also valid for the law of Rompe and Weizel. Braginskiy's constant, in contrast, exhibits a notable rise in the higher current path.

Through the point-by-point evaluation of the discharge current curves, the corresponding spark constants are available as mean

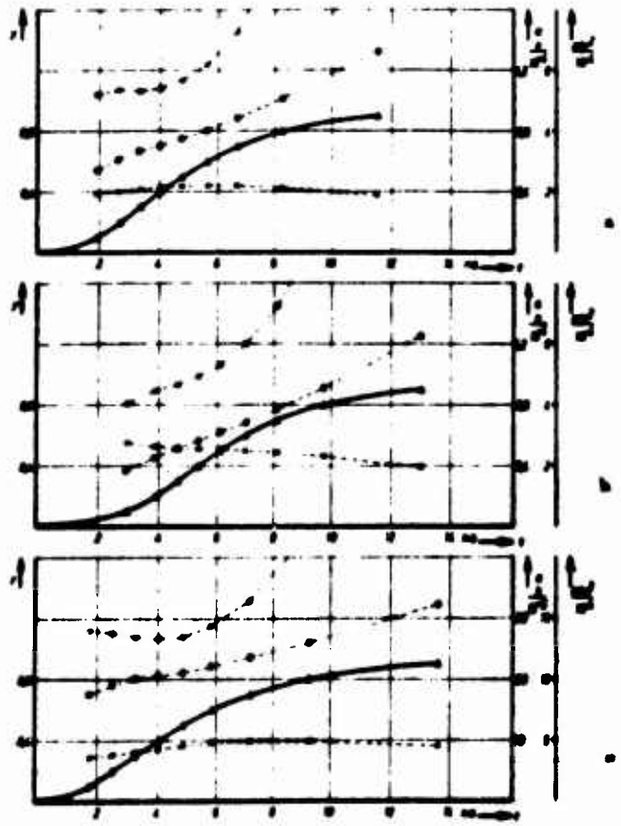

Fig. 6. Progression of the spark constants at s=10 mm and p=2 at; a) filling gas N_2; b) filling gas CO_2; c) filling gas A.

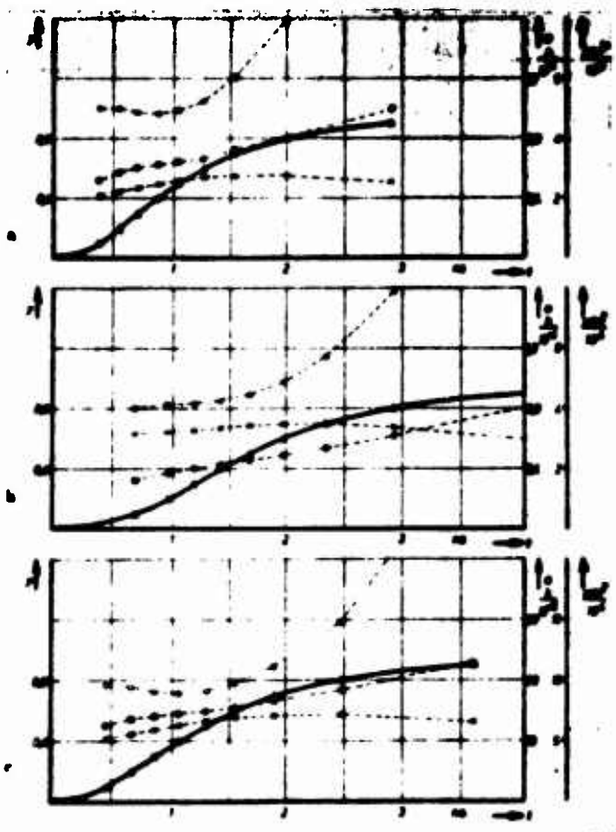

Fig. 7. Progression of the spark constants at s=2 mm and p=11 at. a) filling gas N_2; b) filling gas CO_2; c) filling gas A.

value of the measurement. Thus, with respect to equation (17), the rise time t_{max} of the artificial key wave can also be calculated. Hereby it can be started from the fact that at sufficient accuracy of the individual laws, the values obtained for t_{max} agree to some extent, which is confirmed by the evaluation. During the consideration of the corresponding expressions for t_{max}, it is recognized that this is possible only for variable E_0, so long as the following is valid:

$$\text{[illegible]} \qquad (19)$$

From this it ensues, that even if k is a true constant, the spark constant a is directly dependent on E_0/p. Therefore, for example, if E_0 is strongly reduced at constant pressure by a particular electrode shape [13], then an increase in a is unavoidable. On the other hand, at very small spark gaps E_0/p will rise, whereby the value of a reduces. The spark constant $\pi \cdot b^2$, contrarily is obviously dependent on the height of the maximum discharge current. However, the limitation thereto must be stated that an increase in i_{max} by increase of the gas pressure (E_0/p=const) has no effect on the value of $\pi \cdot b^2$, since b^2 is dependent in the same manner on the gas pressure. Contrarily, if i_{max} is increased by an enlargement of the spark gap at constant pressure or by a greater discharging capacitance, then the value of $\pi \cdot b^2$ also increases. This explains the appropriate measurement results by Moeller [13].

6. Measurement Values of the spark Constants and Comparison of the Spark Laws

The spark constants applied already for the determination of t_{max} are now to be given for all parameter combinations (Fig. 8).

It is shown that the Toepler spark constant is fully independent of the spark gap and only increases weakly with the ignition field strength. Thereby, for flight over-pressure the following typical values can be given

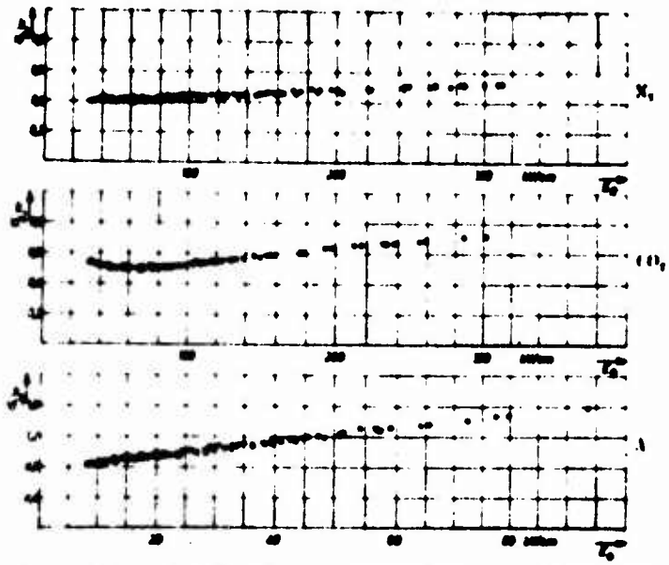

Fig. 8. $k=f(E_0)$, parameter s, K/Vs/cm

Nitrogen	CO_2
$k \approx 0.4 \cdot 10^{-4}$ Vs/cm	$k \approx 0.5 \cdot 10^{-4}$ Vs/cm

Argon

$k \approx 0.85 \cdot 10^{-5}$ Vs/cm.

The values obtained for nitrogen can most validly be compared with the previous measurements in air at normal pressure, and they show quite good agreement.

The progression of the spark constants of Rompe and Weizel is no longer surprising, since noteworthy changes of E_0/p take place in the considered range of measurement (Fig. 9). Therefrom there then results an indirect spark gap dependence of the spark constants. Thereby not only the expected tendency is fulfilled, but rather also the numerical relationships agree well. At average spark gaps the following typical values result

Nitrogen	CO_2
$a \approx 1.1$ at$\cdot$cm^2/V^{2}s	$a \approx 1.0$ at$\cdot$cm^2/V^{2}s

Argon

$a \approx 25$ at$\cdot$cm^2/V^{2}s.

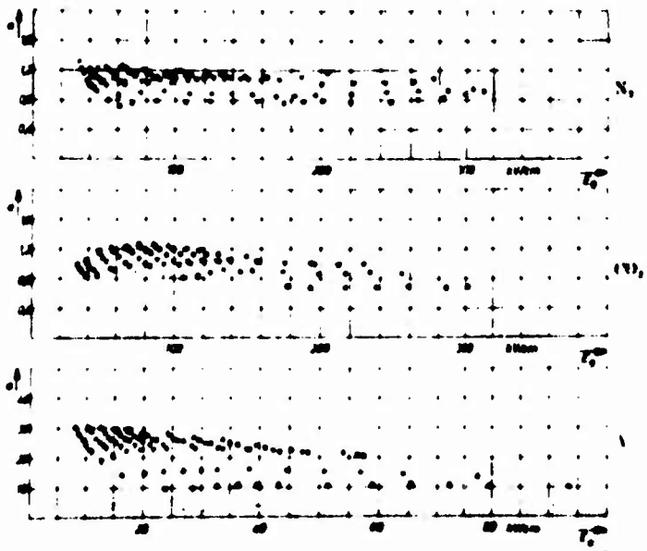

Fig. 9. $a=f(E_0)$, parameter s, $a/at \cdot cm^2/V^2s$.

For nitrogen there again exists good agreement with the previous measurement values for air at normal and over-pressure.

The progression of Braginskiy's spark constants corresponds exactly to the employed considerations (Fig. 10). Accordingly, the occurring spark gap dependence is to be traced back to the simultaneous change of i_{max}. For average spark gaps there result approximately the following numerical values:

Nitrogen	$\approx 3.5 \cdot 10^4$
CO_2	$\approx 3 \cdot 10^4$
Argon	$\approx 1 \cdot 10^4$

The values for nitrogen correspond somewhat to the previous measurements for air and normal pressure. The agreement becomes even better if it is considered that thereby higher discharge currents constantly occur.

It can be concluded from the measurement values of the spark constants that all spark laws in the region of the voltage breakdown are applicable. Therefore it shall now be attempted to retroactively calculate properties of the gases involved at the given conditions

from the measured spark constants. That is directly pcssible only for the constants of Rompe and Weizel. The calculations in the following are conducted constantly for p=1.5, so that a comparison with corresponding measurements at normal pressure is still conductable. If the electron temperature is calculated at $T_e \approx 5 \cdot 10^4$ °K, then the electron mobility is obtained from equation (9) with omission of the excitation energy. Under consideration of these values, then according to equation (7) the effective cross section for ionization can be calculated:

Nitrogen	CO_2
$V_i \sim 16$ V	$V_i \sim 14$ V
$b_e \approx 16.7$ cm²/Vs	$b_e \sim 12.6$ cm²/Vs
$Q_{e,i} \quad 1.5 \cdot 10^{-16}$ cm²	$Q_{e,i} \sim 1.5 \cdot 10^{-16}$ cm²

Argon
$V_i \approx 16$ V
b_e 375 cm² Vs
$Q_{e,i} \approx 0.31 \cdot 10^{-16}$ cm²

It shall now be attempted on the basis of equation (3) to estimate the specific conductance of the spark channel, so as to then calculate the Braginskiy spark constants with the known values of the constants b, and to compare them with the measurement values. For this it is assumed that the degree of ionization amounts to one. For nitrogen and CO_2 two electrons per molecule are to be created and for argon correspondingly only one electron:

Nitrogen	CO_2
$n_e \approx 8.1 \cdot 10^{18}$ cm⁻³	$n_e \approx 8.1 \cdot 10^{18}$ cm⁻³
$\varkappa \approx 215$ S·cm⁻¹	$\varkappa \sim 178$ S·cm⁻¹

Argon
$n_e \approx 4.05 \cdot 10^{18}$ cm⁻³
$\varkappa$ 2430 S·cm⁻¹

The assumptions encountered appear to somewhat correspond to the actual relationships, since for air and normal pressure a value of 300 $S \cdot cm^{-1}$ was derived by Andreev and Orlov [11] and 350 $S \cdot cm^{-1}$ by Moeller [13]. Now it still must be calculated according to the

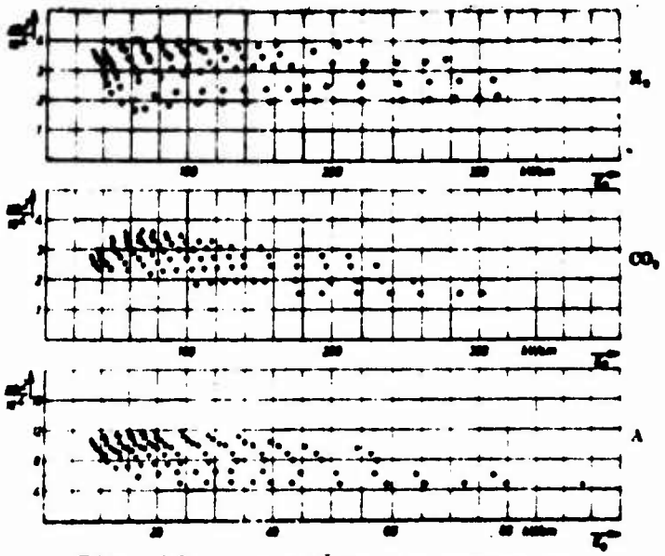

Fig. 10. [illegible]

data of Drabkina [6] and Braginskiy [7] for the constant b.

This is accomplished from equation (11) for K_p=0.9 and c=3/4:

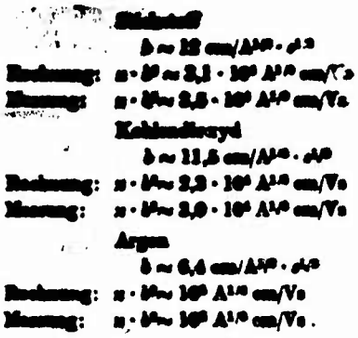

[Stickstoff - Nitrogen; Rechnung - Calculation; Messung - Measurement; Kohlendioxyd - CO_2.]

The agreement is surprisingly good. This again speaks for the fact that all three spark laws are equally valid and differ only in accuracy.

This conclusions cannot be confirmed by the fact that the spark channel radius is calculated according to Braginskiy's theory and is compared with the constant channel radius of the spark model

conducted according to the Toepler Law. In the following that is to be conducted at a point, where a well-conducting spark channel has already been formed (y=0.8). The channel radii involved are obtained from equations (3), (6), and (10):

$$r_{fT} = \sqrt{\frac{Q_w \cdot t_{arc}}{\pi \cdot \varepsilon \cdot \eta_a} \cdot \int y \cdot dt}, \qquad r_{fB} = b \cdot \left(\frac{Q_w}{\varepsilon}\right)^{0,6} \cdot \sqrt{\int y^{0,6} \cdot dt}. \qquad (20)$$

	$\varepsilon = 10$ mm	$\varepsilon = 5$ mm
Nitrogen	$r_{fT} = 0{,}111$ mm	$r_{fT} = 0{,}077$ mm
	$r_{fB} = 0{,}100$ mm	$r_{fB} = 0{,}076$ mm
CO_2	$r_{fT} = 0{,}120$ mm	$r_{fT} = 0{,}086$ mm
	$r_{fB} = 0{,}106$ mm	$r_{fB} = 0{,}082$ mm
Argon	$r_{fT} = 0{,}032$ mm	$r_{fT} = 0{,}022$ mm
	$r_{fB} = 0{,}031$ mm	$r_{fB} = 0{,}024$ mm

	$\varepsilon = 1$ mm
Nitrogen	$r_{fT} = 0{,}034$ mm
	$r_{fB} = 0{,}042$ mm
CO_2	r_{fT} not calculable
	r_{fB} due to step formation*
Argon	$r_{fT} = 0{,}009$ mm
	$r_{fB} = 0{,}013$ mm.

The agreement is so good that no doubt can exist anymore on the equivalent validity of the spark laws in the region of the voltage breakdown.

I thank Professor Dr. of Engineering Gerhard Fruehauf and Professor Dr. of Engineering Wolfram Boeck for the constant interest in this work.

*It will be reported separately concerning the step formation which occurs under certain conditions during spark discharges in CO_2

BIBLIOGRAPHY

[1] Toepler, M.: ETZ 48, 1046 (1926). — [2] Möller, H.: Archiv Elektrot. 18, 288 (1927). — [3] Toepler, M.: Archiv. Elektrot. 18, 563 (1927). — [4] Rompe, R., Weizel, W.: Über das Toeplersche Funkengesetz. Zeitschr. Phys. 122, 636 (1944). — [5] Rompe, R., Weizel, W.: Theorie des elektrischen Funkens. Ann. Phys. 6. Folge 1, 285 (1947). — [6] Drabkina, S. I.: Zur Theorie der Entwicklung des Funkenkanals. Abh. sowj. Phys. 2, 295 (1953). — [7] Braginskii, S. I.: Theory of the development of a spark channel. Soviet Physics JETP 7, 1068 (1958). — [8] Andreev, S. I., Vanyukov, M. P.: Application of a spark discharge to obtain intense light flashes of length 10^{-7}—10^{-6} second. I. Investigation of electrical processes in a spark discharge of nanosecond duration. Soviet Physics, Techn. Physics 6, 709 (1962). — [9] Andreev, S. I., Vanyukov, M. P., Kotsiov, A. B.: Growth of the spark discharge canal for a discharge circuit with a rapidly increasing current. Soviet Physics, Techn. Physics 7, 37 (1962). — [10] Grünberg, R.: Gesetzmäßigkeiten von Funkenentladungen im Nanosekundenbereich. Z. Naturf. 20a, 208 (1965). — [11] Andreev, S. I., Orlov, B. I.: Development of a spark discharge. Soviet Physics, Techn. Physics 10, 1097 (1966). — [12] Hochsteuer, F., Kärner, H.: Ein Verfahren zur digitalen Bewertung der Spannungszusammenbrüche von Funkenstrecken. ETZ-A 89, 101 (1968). — [13] Möller, K.: Untersuchung über den zeitlichen Verlauf von Funkenentladungen in Luft. Habilitationsschrift, TH Darmstadt 1968. — [14] Mesyats, G. A., Kozhevnov, G. S.: Formation of nanosecond sparks in static breakdown of a gap. Soviet Physics, Techn. Physics 13, 488 (1968). — [15] Pfeiffer, W.: Aufbau und Überprüfung von koaxialen Rohrwiderständen sehr kurzer Anstiegszeit. ETZ-A 91, 59 (1970). — [16] Gänger, B.: Der elektrische Durchschlag von Gasen. Berlin-Göttingen-Heidelberg: Springer 1955.

Dipl.-Ing. Wolfgang Pfeiffer
Institut für Hochspannungs- und Meßtechnik
der Technischen Hochschule
D - 6100 Darmstadt
Deutschland